

## Stability of the Spontaneous Quantum Hall State in the Triangular Kondo-Lattice Model

Yasuyuki Kato, Ivar Martin, and C. D. Batista

*Theoretical Division, Los Alamos National Laboratory, Los Alamos, New Mexico 87545, USA*

(Received 15 September 2010; published 27 December 2010)

We study the behavior of the quarter-filled Kondo-lattice model on a triangular lattice by combining a zero-temperature variational approach and finite-temperature Monte Carlo simulations. For intermediate coupling between itinerant electrons and classical moments  $\mathbf{S}_j$ , we find a thermodynamic phase transition into an exotic spin ordering with uniform scalar spin chirality and  $\langle \mathbf{S}_j \rangle = 0$ . The state exhibits a spontaneous quantum Hall effect. We also study how its properties are affected by the application of an external magnetic field.

DOI: 10.1103/PhysRevLett.105.266405

PACS numbers: 71.10.Fd, 71.27.+a, 73.43.-f

The very broad spectrum of physical phases and responses of strongly correlated materials is rooted in the simple fact that electrons carry both charge and spin. The interplay between these degrees of freedom gives rise to unconventional forms of superconductivity, multiferroic behavior, giant magnetoresistance, and heavy fermion physics. It also entails the possibility of strong magnetoelectric effects. In insulators, the electric polarization can be induced or modified with a magnetic field, or by coupling to certain magnetic orderings [1]. In metallic systems, the magnetoelectric effects are manifested in the conductivity tensor. The giant [2,3] and colossal [4] magnetoresistance effects are examples in which the diagonal part of the conductivity tensor is dramatically modified. In addition, magnetic ordering can lead to changes in the off-diagonal components. For instance, the “anomalous Hall effect” observed in the presence of ferromagnetic order, even in the absence of an external magnetic field, has been the subject of active research over the past several decades [5–7].

Recently, a residual Hall effect was observed in the absence of both magnetic field and uniform magnetization in the metallic pyrochlore  $\text{Pr}_2\text{Ir}_2\text{O}_7$  [8]. This observation suggests that the effect is caused by a magnetic structure with nonzero average scalar spin chirality, which for a single triangular plaquette is  $\langle \chi_{ijk} \rangle = \langle \mathbf{S}_i \cdot \mathbf{S}_j \times \mathbf{S}_k \rangle$  [9]. Scalar spin chirality breaks time reversal and parity symmetries and can be stabilized even in the absence of usual magnetic ordering:  $\langle \mathbf{S}_i \rangle = 0$  [10]. The symmetry properties of this order parameter lead to unusual magnetoelectric effects in metals [9,11–15] and in insulators [16]. The origin of the magnetoelectric coupling lies in the Berry phase [17] that electrons accumulate as they traverse closed paths in the real space. The Berry phase is half of the solid angle subtended by the electron spin as it moves around the path; e.g., in the continuum limit of smooth magnetic textures, it is proportional to the integral of the scalar spin chirality (or Berry curvature) over the area enclosed by the loop. For a given spin species (locally parallel or antiparallel to the magnetic texture), the effect

of the Berry phase is equivalent to an orbital coupling to a magnetic field. Therefore, it can lead to finite Hall conductivity even in the absence of an external magnetic field.

Under the special circumstances of commensuration between the strength of the effective magnetic field (i.e., Berry curvature of magnetic texture) and the itinerant electron density in quasi-2D systems, there is an exciting possibility of obtaining a spontaneous quantum Hall effect (SQHE), i.e., quantized Hall response for zero magnetic field and zero uniform spin polarization. In a recent work [11], we have shown that such an insulating chiral phase is indeed stabilized at zero temperature,  $T = 0$ , in the weak-coupling regime of a triangular Kondo lattice model (KLM) for a  $3/4$  filled conduction band ( $\rho = 3/4$ ). This result was based on the perfect nesting properties of the noninteracting Fermi surface for  $\rho = 3/4$ , which leads to a “3Q ordering” of the classical local moments at  $T = 0$ .

In the present Letter we explore the stability of chiral order in a 2D KLM with respect to thermal fluctuations and magnetic fields. It is well known that a continuous symmetry cannot be broken at finite temperature in 2D when the interactions are of short range [18]. However, a noncoplanar magnetic ordering breaks a discrete  $Z_2$  symmetry, in addition to the continuous symmetry, that corresponds to the two disconnected  $\text{SO}(3)$  sectors of  $\text{O}(3)$  rotations needed to parametrize the order parameter [19,20]. The Ising component of this order parameter (chirality) can survive at finite temperature leading to a chiral spin-liquid:  $\langle \chi_{ijk} \rangle \neq 0$  and  $\langle \mathbf{S}_j \rangle = 0$ . The interplay between the continuous and the Ising degrees of freedom in such a chiral liquid is nontrivial and can lead to deviations from the Ising universality class and a reduction of the transition temperature [21,22].

To study this problem we combined a zero-temperature variational approach with finite-temperature Monte Carlo (MC) simulations [23] of the KLM with classical local moments. We demonstrate that the 3Q phase with uniform chirality (UCP) of Ref. [11] is stable not only at  $\rho = 3/4$ , but also at  $\rho = 1/4$  in the intermediate coupling regime  $1 \lesssim J/t \lesssim 4$  ( $t$  is the hopping amplitude for the conduction

electrons and  $J$  is their exchange coupling to the localized moments). This result agrees with the small-unit cell variational calculations at  $T = 0$  presented in Ref. [24]. Our MC results provide evidence for a first order thermodynamic phase transition into the UCP. The obtained ordering temperature at  $J = 2t$ ,  $T_c \simeq 0.03t$ , is relatively small compared to  $J$  and  $t$ , likely because of the strong frustration and the suppression of the chiral order by the continuous fluctuations of magnetization. Nevertheless, the value of  $T_c$  may be high enough for observing SQHE near room temperature in transition metal oxides (assuming that  $t$  is of order 1 eV [25]). Finally, we consider the effect of a magnetic field acting on the local moments both on the stability of the  $T = 0$  UCP phase and the spontaneous quantum Hall effect, as well as on the value of  $T_c$ .

We consider the Kondo-lattice Hamiltonian on a triangular lattice with periodic boundary conditions,

$$\mathcal{H} = -t \sum_{\langle l,j \rangle \sigma} (c_{l\sigma}^\dagger c_{j\sigma} + \text{H.c.}) - J \sum_{j\mu\nu} \mathbf{S}_j \cdot c_{j\mu}^\dagger \boldsymbol{\sigma}_{\mu\nu} c_{j\nu}$$

where  $c_{j\sigma}^\dagger$  ( $c_{j\sigma}$ ) is the creation (annihilation) operator of an electron with spin  $\sigma$  on site  $j$ ,  $\mathbf{S}_j$  is a classical Heisenberg spin with  $|\mathbf{S}_j| = 1$ ,  $\boldsymbol{\sigma}_{\mu\nu} = (\sigma_{\mu\nu}^x, \sigma_{\mu\nu}^y, \sigma_{\mu\nu}^z)$  is a vector of Pauli matrices, and  $\langle l, j \rangle$  indicates that  $l$  and  $j$  are nearest-neighbor sites. Since the sign of  $J$  is irrelevant for classical moments,  $\mathbf{S}_j$ , we will assume  $J > 0$  for concreteness.

The state of interest is characterized by the local scalar spin chirality  $\chi_{ijk} \equiv \mathbf{S}_i \cdot \mathbf{S}_j \times \mathbf{S}_k$ , and its Fourier transform

$$\chi_{\mathbf{q}} = N^{-1} \sum_{\alpha} \chi_{\alpha} e^{i\mathbf{q} \cdot \mathbf{r}_{\alpha}}. \quad (1)$$

The index  $\alpha$  denotes each triangular plaquette, and  $N = L^2$  is the total number of lattice sites. The global order parameter for the UCP is  $\langle \chi_0 \rangle$ . Local spin correlations are described by the spin structure factor

$$S(\mathbf{k}) = N^{-1} \sum_{j,l} \langle \mathbf{S}_j \cdot \mathbf{S}_l \rangle e^{i\mathbf{k} \cdot (\mathbf{r}_l - \mathbf{r}_j)}, \quad (2)$$

which is useful for characterization of the  $T = 0$  spin ordering. We note here that for the perfectly ordered UCP, which is the same as the ‘‘all-out’’ phase in Fig. 1, simple arithmetic shows that  $\chi_0^2 \simeq 0.59$  and  $S(\mathbf{0}) = 0$ , while  $\chi_{\mathbf{q}}^2 = 0$  and  $S(\mathbf{0}) = N$  for the fully polarized ferromagnetic state.

The MC simulation samples the space of all possible classical spin configurations. For each configuration  $\{\mathbf{S}\}$ , the electron eigenstates are found by exact diagonalization of  $\mathcal{H}$ . To study the thermodynamic properties at a fixed filling factor  $\rho$ , we perform a Legendre transformation of the free energy in the grand canonical ensemble. The resulting free energy is

$$F(N, \beta) \equiv -\frac{1}{\beta} \ln \Xi, \quad \Xi \equiv \sum_{\{\mathbf{S}\}} W(\{\mathbf{S}\}), \quad (3)$$

with  $W(\{\mathbf{S}\}) \equiv e^{-\beta \mu_{\{\mathbf{S}\}} N_e} \prod_{\lambda} [1 + e^{-\beta \epsilon_{\lambda} - \mu_{\{\mathbf{S}\}}}]$ . The chemical potential  $\mu_{\{\mathbf{S}\}}$  is adjusted for a given configuration  $\{\mathbf{S}\}$  such that the total number of electrons,  $N_e = \sum_{\lambda} f_{\lambda}$ , is the

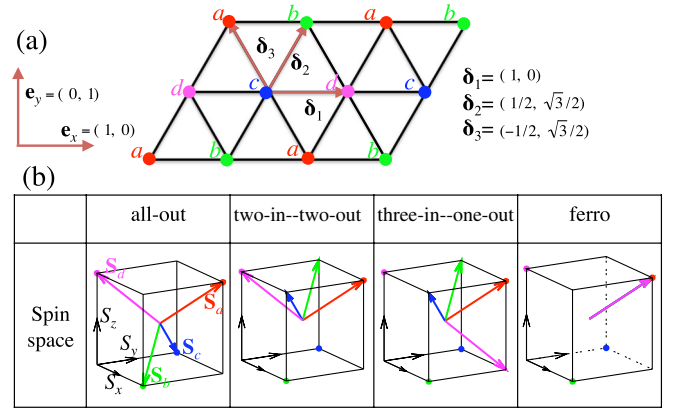


FIG. 1 (color online). The four-sublattice spin structures. (a) Triangular lattice, with  $a - d$  indicating each sublattice. (b) High-symmetry four-sublattice spin structures. The nomenclature follows the one for magnetic ordering on a tetrahedron with vertices  $(abcd)$ .

same for every spin configuration. Here,  $\epsilon_{\lambda}$  is the  $\lambda$ th eigenvalue of  $\mathcal{H}(\{\mathbf{S}\})$ ,  $f_{\lambda} \equiv (e^{\beta \epsilon_{\lambda} - \mu_{\{\mathbf{S}\}}} + 1)^{-1}$ , and  $\beta = 1/T$ . In this work we compute the energy density,  $\epsilon \equiv N^{-1} \partial_{\beta}(\beta F)$ , and the specific heat,  $c \equiv \partial_T \epsilon$ . Our numerical results are based on the single spin flip MC dynamics, with the flip decided by applying the Metropolis algorithm. We perform 10 000 MC sweeps for each processor and estimate the statistical errors using 8 mean values typically.

First we consider the  $T = 0$  case by means of a variational calculation in which we minimize the total energy over several highly symmetric four-sublattice spin structures shown in Fig. 1 [26]. The all-out and ferromagnetic configurations are the only two states that are stabilized as a function of  $J/t$  for  $\rho = 1/4$ . Figure 2(a) includes a comparison between the corresponding energy densities  $\epsilon(\{\mathbf{S}\}) \equiv L^{-2} \sum_{\lambda} \epsilon_{\lambda} f_{\lambda}$  for  $\rho = 1/4$ . The solid lines are the results for  $L = 512$ . The all-out structure has the lowest energy for  $0 < J/t \lesssim 4.9$ , while the ferromagnetic

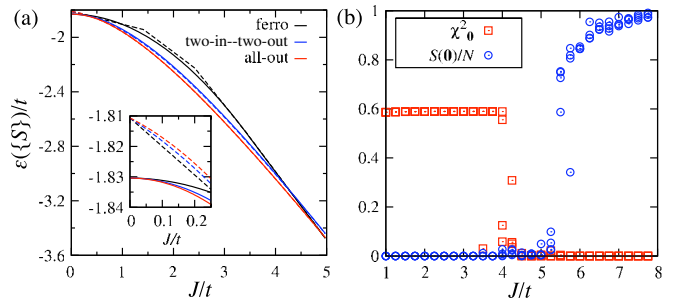


FIG. 2 (color online). (a) Energy per site as a function of  $J/t$  for the all-out, two-in-two-out, and ferromagnetic spin structures at  $\rho = 1/4$  for  $L = 512$  (solid line) and  $L = 8$  (dashed line). Insets show an enlarged view for small  $J/t$ . (b) Coupling  $J/t$  dependence of  $\chi_0^2$  and  $S(\mathbf{0})$  at quarter filling by Monte Carlo method with  $L = 8$  and very low temperature  $T/t = 10^{-4}$ . Four mean values of  $\chi_0^2$  and  $S(\mathbf{0})$  are shown for each value of  $J/t$  to indicate the lack of convergence the MC simulation in the interval the phase transition,  $4 \lesssim J/t \lesssim 6$ .

configuration becomes the minimum energy state for  $J/t \gtrsim 4.9$ . A similar comparison for  $L = 8$  (dashed lines) indicates that important size effects appear in the weak coupling regime,  $J/t \lesssim 1$ , for small values of  $N$  [see the inset of Fig. 2(a)]. The energy of the ferromagnetic structure is lower than the energy of the all-out structure for  $L = 8$  and small values of  $J/t < 1$ , although this is not true in the thermodynamic limit. The all-out structure, which is the lowest energy variational state for  $J/t \lesssim 4.9$ , has a net uniform scalar spin chirality. Therefore, it has to produce a spontaneous Hall effect. By explicit calculation of the Hall conductivity from the electron band structure, we find the quantized value  $\sigma_{xy} = \pm e^2/h$  for  $0.7 \lesssim J/t \lesssim 4.9$ .

Not being limited to the  $2 \times 2$  magnetic unit cell size, the low temperature MC calculations allow us to test the variational approach. Figure 2(b) shows our MC results for the  $J/t$  dependence of  $\chi_0^2$  and  $S(\mathbf{0})$  at  $T/t = 10^{-4}$  and  $L = 8$ . These results indicate that the all-out spin structure with uniform scalar chirality is indeed stable for  $J/t \lesssim 4$ , while the ferromagnetic phase is stabilized for  $J/t \gtrsim 5$  (the long range magnetic ordering is stable only at  $T = 0$ ). Our MC simulation does not converge at these very low temperatures in the interval  $4 \lesssim J/t \lesssim 6$ . We traced the lack of convergence to an intervening spiral phase, which in the  $L = 8$  lattice is slightly lower in energy than the fully polarized and the all-out phases for  $4.9 \lesssim J/t \lesssim 6.3$ . However, the spiral becomes unstable for larger lattices ( $L > 64$ ). Therefore, we conclude that the nonconvergent window between the all-out and the fully polarized phases is only a finite size effect, and there is a direct transition from the all-out to the ferromagnetic phase as a function of  $J/t$  [24]. We also find that  $S(\mathbf{0})$  is finite while  $\chi_0^2$  is almost zero below  $J/t \sim 0.5$ . This is a consequence of the finite size effect that was already discussed in our variational calculation [see Fig. 2(a)]. The intermediate coupling range,  $1 < J/t < 4$ , appears to be stable against size effects.

We now turn to the question of the finite temperature stability of the chiral magnetic phase. Our main results are presented in Fig. 3. To control the size effects, we varied  $L$  at fixed coupling strength  $J/t = 2$ . This value of  $J/t$  gives a robust all-out chiral ordering at  $T = 0$ . As expected from the simple Ising argument in 2D, this chiral ordering should persist for a finite range of temperatures. Starting from the maximum possible value at  $T = 0$ , the scalar chirality decreases as a function of  $T$  and vanishes at  $T_c \simeq 0.026t$ . The snapshot of a spin configuration at  $T = 0.005t$  in Fig. 3(b) illustrates how the finite-temperature fluctuations destabilize the chiral ordering. The temperature dependence of the spin-spin and chirality-chirality correlation functions (not shown in this paper) are also consistent with chiral ordering without spin ordering. The calculated specific heat curve exhibits a very sharp and symmetric peak at  $T_c$ , which is an indication of a first order transition. To test this possibility, we analyzed the temperature dependence of the internal energy probability distribution [Fig. 3(c)]. We found that it has a

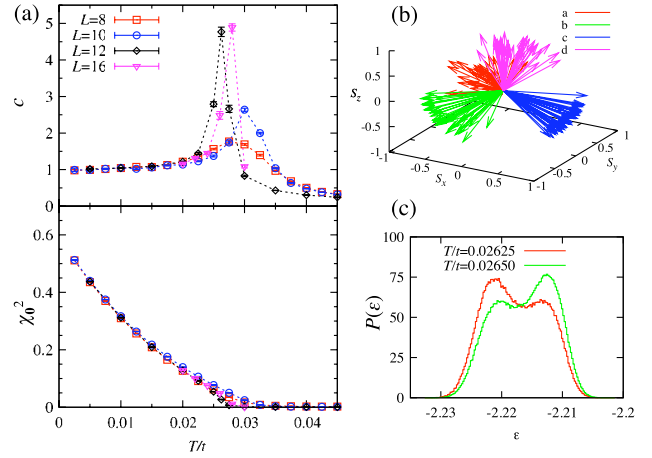


FIG. 3 (color online). Results of Monte Carlo simulations at quarter filling and  $J/t = 2$ . (a) Temperature dependence of specific heat  $c$  and  $\chi_0^2$ . (b) Snapshot of a spin configuration. Each shade (color) corresponds to each of the four different sublattices ( $L = 12$ ,  $T/t = 0.005$ ). (c) Internal energy distribution near the critical temperature for  $L = 12$ .

bimodal distribution for  $T$  near  $T_c$  and  $L = 12$ . In combination with the specific heat behavior, this result indicates that the thermodynamic phase transition between the paramagnetic and the chiral all-out state is of the first order.

The magnetic field,  $\mathbf{h}$ , is an important parameter that can be used to control the chiral magnetic states. It couples to both local and itinerant electron spins, as well as to the orbital motion of electrons, and hence can lead to a variety of phases. For simplicity, here we only consider the Zeeman coupling to the local moments,  $\mathcal{H}_z = -\sum_j \mathbf{H} \cdot \mathbf{S}_j$ , with  $\mathbf{H} \equiv g\mu_B \mathbf{S} \mathbf{h} = H\hat{z}$ , and neglect the coupling to the conduction electrons ( $S$  is spin of the localized moments). This approximation is justified for  $S \gg 1$  because the Pauli susceptibility becomes much smaller than the local moment susceptibility, while the orbital effect of Berry curvature induced by the magnetic texture dominates over the orbital effect of  $\mathbf{h}$ .

The  $T = 0$  variational approach for  $J/t = 2$  reveals that the all-out structure is distorted by the field in the way that

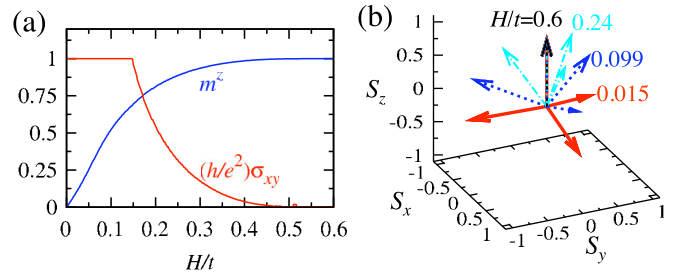


FIG. 4 (color online). Variational calculation of the ground state of  $\mathcal{H} + \mathcal{H}_z$  by minimizing the energy over several highly symmetric four-sublattice spin configurations ( $L = 2048$ ): (a) Hall conductance,  $\sigma_{xy}$ , and uniform magnetization along the field direction,  $m^z$ , as a function of the applied magnetic field  $H/t$ . (b) Field dependence of the four-sublattice spin structure of the variational ground state.



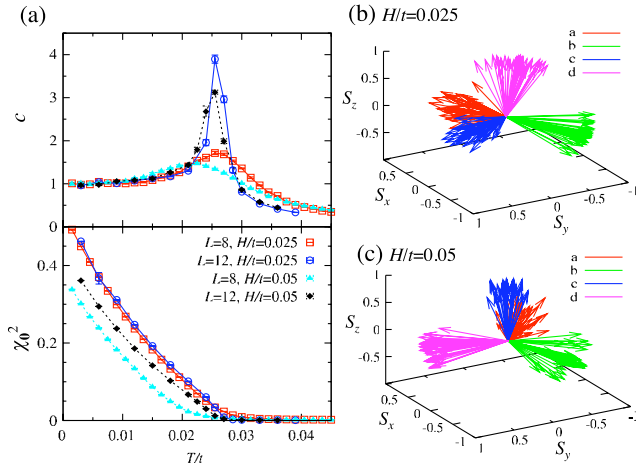


FIG. 5 (color online). Results of Monte Carlo simulation at quarter filling and  $J/t = 2$ , for two values of applied magnetic field,  $H/t = 0.025$  and  $0.05$ . (a) Temperature dependence of specific heat  $c$  and  $\chi_0^2$ . (b),(c) Configurations of all spins classified according to sublattice ( $L = 12$ ,  $T/t = 0.003$ ), with (b)  $H/t = 0.025$  and (c)  $H/t = 0.05$ .

interpolates between the all-out and three-in-one-out structure [Fig. 1(b)], until it saturates at  $H_{\text{sat}} \approx 0.5t$  as shown in Fig. 4(b). The spins of one of the four sublattices are always aligned with the field direction. The gap in the electron spectrum closes at the critical field  $H_c/t \approx 0.15$  leading to an insulator-to-metal transition. Correspondingly,  $\sigma_{xy}$ , starts to decrease continuously at  $H = H_c$ , from its quantized value for  $H \leq H_c$  to zero for  $H \geq H_{\text{sat}}$ . In this way, the application of an external field suppresses SQHE in the insulating state by inducing a metallic phase with anomalous Hall effect.

We performed MC simulations in the low field region,  $H = 0.025t$  and  $H = 0.05t$ , for  $L = 8$  and  $L = 12$  (for larger values of  $H$  the variational approach revealed spurious finite size effects in systems with  $L < 64$ ). The results are shown in Fig. 5. The position of the specific heat peak [Fig. 5(a)] and the onset of the chiral order parameter [Fig. 5(a)] indicate that the transition temperature to the chiral phase is suppressed by the presence of the magnetic field. The snapshots of the spin configurations in each sublattice (identified with color) show a result that is consistent with the variational approach: the spins are canted towards the three-in-one-out configuration, with one of the spin sublattices tending to be aligned with the applied field [see Figs. 5(b) and 5(c)]. The fluctuations around this preferred orientation decrease with increasing  $H$ .

In summary, we have demonstrated the finite-temperature stability of a chiral spin liquid in a Kondo lattice model. This liquid exhibits a spontaneous quantum Hall effect, which can be tuned by an external magnetic field. The phase exists in a wide range of Hund's coupling strengths and can therefore be realized, e.g., in manganese-based materials [25]. Even though we did not include the effect of quantum fluctuations, the chiral phase is expected

to be stable for  $S \gg 1$ . In the quantum limit  $S = 1/2$ , it may also be relevant to  $\text{Na}_{0.5}\text{CoO}_2$  [11,27].

We thank S. Nakatsuji and Y. Motome for useful discussions. This work was carried out under the auspices of the NNSA of the U.S. DOE at LANL under Contract No. DE-AC52-06NA25396 and supported by the LANL/LDRD Program. This research used resources of the NERSC Center.

- [1] Y. Tokura, *Science* **312**, 1481 (2006).
- [2] M. N. Baibich, J. M. Broto, A. Fert, F. Nguyen Van Dau, F. Petroff, P. Etienne, G. Creuzet, A. Friederich, and J. Chazelas, *Phys. Rev. Lett.* **61**, 2472 (1988).
- [3] G. Binash, P. Grünberg, F. Saurenbach, and W. Zinn, *Phys. Rev. B* **39**, 4828 (1989).
- [4] J. Lalena and D. Cleary, *Principles of Inorganic Materials Design* (John Wiley and Sons, New York, 2010), 2nd ed.
- [5] N. Sinitsyn, *J. Phys. Condens. Matter* **20**, 023201 (2008).
- [6] N. Nagaosa, J. Sinova, S. Onoda, A. H. MacDonald, and N. P. Ong, *Rev. Mod. Phys.* **82**, 1539 (2010).
- [7] D. Xiao, M.-C. Chang, and Q. Niu, *Rev. Mod. Phys.* **82**, 1959 (2010).
- [8] Y. Machida, S. Nakatsuji, S. Onoda, T. Tayama, and T. Sakakibara, *Nature (London)* **463**, 210 (2010).
- [9] K. Ohgushi, S. Murakami, and N. Nagaosa, *Phys. Rev. B* **62**, R6065 (2000).
- [10] J.-C. Domenge, P. Sindzingre, C. Lhuillier, and L. Pierre, *Phys. Rev. B* **72**, 024433 (2005).
- [11] I. Martin and C. D. Batista, *Phys. Rev. Lett.* **101**, 156402 (2008).
- [12] R. Shindou and N. Nagaosa, *Phys. Rev. Lett.* **87**, 116801 (2001).
- [13] Y. Taguchi, Y. Oohara, H. Yoshizawa, N. Nagaosa, and Y. Tokura, *Science* **291**, 2573 (2001).
- [14] A. Neubauer, C. Pfleiderer, B. Binz, A. Rosch, R. Ritz, P. G. Niklowitz, and P. Böni, *Phys. Rev. Lett.* **102**, 186602 (2009).
- [15] M. Lee, W. Kang, Y. Onose, Y. Tokura, and N. P. Ong, *Phys. Rev. Lett.* **102**, 186601 (2009).
- [16] L. N. Bulaevskii, C. D. Batista, M. V. Mostovoy, and D. I. Khomskii, *Phys. Rev. B* **78**, 024402 (2008).
- [17] M. Berry, *Proc. R. Soc. A* **392**, 45 (1984).
- [18] N. Mermin and H. Wagner, *Phys. Rev. Lett.* **17**, 1133 (1966).
- [19] J. Villain, *J. Phys. (Les Ulis, Fr.)* **38**, 385 (1977).
- [20] H. Kawamura and S. Miyashita, *J. Phys. Soc. Jpn.* **53**, 4138 (1984).
- [21] T. Momoi, K. Kubo, and K. Niki, *Phys. Rev. Lett.* **79**, 2081 (1997).
- [22] J.-C. Domenge, C. Lhuillier, L. Messio, L. Pierre, and P. Viot, *Phys. Rev. B* **77**, 172413 (2008).
- [23] G. Alvarez, M. Mayr, and E. Dagotto, *Phys. Rev. Lett.* **89**, 277202 (2002).
- [24] Y. Akagi and Y. Motome, *J. Phys. Soc. Jpn.* **79**, 083711 (2010).
- [25] E. Dagotto, *Nanoscale Phase Separation and Colossal Magnetoresistance* (Springer, Berlin, 2003), 1st ed.
- [26] See Ref. [24] for a more exhaustive variational approach.
- [27] T. Li, [arXiv:1001.0620](https://arxiv.org/abs/1001.0620).